Article No. jmbi.1999.3218 available online at http://www.idealibrary.com on IDEAL® J. Mol. Biol. (1999) 293, 1241–1255

JMB

Salt Bridge Stability in Monomeric Proteins

Sandeep Kumar[1] and Ruth Nussinov[2,3]*

[1]*Laboratory of Experimental and Computational Biology Bldg 469, Rm 151, National Cancer Institute, Frederick Cancer Research and Development Center, Frederick MD 21702, USA*

[2]*Intramural Research Support Program, SAIC Frederick Laboratory of Experimental and Computational Biology Bldg 469, Rm 151, National Cancer Institute, Frederick Cancer Research and Development Center, Frederick, MD 21702, USA*

[3]*Sackler Institute of Molecular Medicine, Sackler School of Medicine, Tel Aviv University Tel Aviv, 69978, Israel*

**Corresponding author*

Here, we present the results of continuum electrostatic calculations on a dataset of 222 non-equivalent salt bridges derived from 36 non-homologous high-resolution monomeric protein crystal structures. Most of the salt bridges in our dataset are stabilizing, regardless of whether they are buried or exposed, isolated or networked, hydrogen bonded or non-hydrogen bonded. One-third of the salt bridges in our dataset are buried in the protein core, with the remainder exposed to the solvent. The difference in the dielectric properties of water *versus* the hydrophobic protein interior cost buried salt bridges large desolvation penalties. However, the electrostatic interactions both between the salt-bridging side-chains, and between the salt bridges and charges in their protein surroundings, are also stronger in the interior, due to the absence of solvent screening. Even large desolvation penalties for burying salt bridges are frequently more than compensated for, primarily by the electrostatic interactions between the salt-bridging side-chains. In networked salt bridges both types of electrostatic interactions, those between the salt-bridging side-chains, and those between the salt bridge and its protein environment, are of similar magnitudes. In particular, a major finding of this work is that salt bridge geometry is a critical factor in determining salt bridge stability. Salt bridges with favorable geometrical positioning of the interacting side-chain charged groups are likely to be stabilizing anywhere in the protein structure. We further find that most of the salt bridges are formed between residues that are relatively near each other in the sequence.

Keywords: stability; salt bridge; electrostatics; geometry; hierarchical folding

Introduction

In folded proteins, pairs of neighboring, oppositely charged residues often interact to form salt bridges. Salt bridges play important roles in protein structure and function such as in oligomerization, molecular recognition, allosteric regulation, domain motions, and α-helix capping (Perutz, 1970; Fersht, 1972; Barlow & Thornton, 1983; Musafia *et al*., 1995; Xu *et al*., 1997a,b; Kumar *et al*., 1999). Based on conventional biochemical intuition, one would expect salt bridges to be stabilizing towards the folded conformations of proteins. Yet estimates of the electrostatic contribution to the free energy change upon salt bridge formation vary significantly. Experimental as well as theoretical estimates of the electrostatic free energy contribution of the salt bridges range from being stabilizing (Horovitz & Fersht, 1992; Marqusee & Sauer, 1994; Pervushin *et al*., 1996; Lounnas & Wade, 1997; Xu *et al*., 1997b), to being insignificant (Singh, 1988; Serrano *et al*., 1990; Barril *et al*., 1998), to being destabilizing (Sun *et al*., 1991; Dao-pin *et al*., 1991; Hendsch & Tidor, 1994; Waldburger *et al*., 1995). Formation of buried salt bridges has been proposed to be a slow step in protein folding (Waldburger *et al*., 1996). An early calculation by Honig & Hubbell (1984) estimated that the cost of transferring a salt bridge from water to the protein environment is approximately 10-16 kcal/mol. Using continuum electrostatic calculations, it has been shown that the desolvation penalty due to the burial of polar and charged groups in the protein interior (a low dielectric environment) during protein folding, may not be fully recovered by favorable electrostatic interactions in the folded state (Hendsch & Tidor, 1994). Experimental support for this notion is also available (Waldburger *et al*., 1995). However, based on continuum electro-

E-mail address of the corresponding author: ruthn@ncifcrf.gov

0022-2836/99/451241–15 $30.00/0

static calculations, highly stabilizing salt bridges have been reported both within protein monomers (Lounnas & Wade, 1997) and across subunit interfaces (Xu *et al*., 1997b). Using site directed mutagenesis, Kawamura *et al*. (1997) have shown that disruption of the Glu34-Lys38 salt bridge in a DNA-binding protein, HU from *Bacillus stearothermophilus*, reduced its thermal stability. Introduction of this salt bridge into a homologous HU from the mesophile *Bacillus subtilis*, increased the stability of the protein. It has been consistently observed that salt bridges are more frequent in proteins from thermophiles as compared to those from mesophiles (Yip *et al*., 1998; Kumar *et al*., 1999). Theoretical studies on individual or on a small number of proteins have suggested that salt bridges may contribute substantially to protein stability in thermophiles (Kumar *et al*., 1999; Elcock, 1998). Experimentally, surface salt bridges have been shown to stabilize the GCN4 leucine zipper (Spek *et al*., 1998).

Here, our goals were twofold. First, we wanted to determine whether there are general trends in the electrostatic contributions to the free energy change upon salt bridge formation, second, we examined the factors contributing to salt bridge stability. These factors include the location of the bridge in the protein; the positioning of the charged groups of the residues forming the salt bridge with respect to each other; and the chemical nature of neighboring residues and the homogeneity of the protein matrix around the salt bridge. Residues involved in surface salt bridges are expected to pay lower desolvation energy penalties as compared to those involved in buried salt bridges (Hendsch & Tidor, 1994). The interactions between charged groups in the salt-bridging residues can be sensitive to distance and to angular orientation of the charged groups with respect to each other. The electrostatic stability of the bridge may also be affected by the presence of other charged residues in its vicinity. Neighboring charged groups may interact with the salt bridge if they are close enough in space. In such a case, stabilizing salt bridge networks may be formed as in hyperthermophilic glutamate dehydrgenase (Kumar *et al*., 1999). At the same time, the presence of these charges may increase the effective local dielectric constant, providing electrostatic screening.

Below we describe results obtained from continuum electrostatic energy calculations performed on 222 non-equivalent salt bridges derived from 36 monomeric proteins with non-homologous sequences and structures. Three-dimensional structures of these proteins have been solved to high resolution (1.6 Å or better) by X-ray crystallography and are available in the protein data bank (PDB) (Bernstein *et al*., 1977). In particular, these proteins are biologically active as monomers. Furthermore, we present a general statistical survey of the characteristics of the salt bridges. The majority of the salt bridges are exposed; approximately one third of the salt bridges in the dataset are buried in the protein core.

Salt bridges can be stabilizing or destabilizing. Most of the salt bridges in our dataset are stabilizing. Salt bridges with good geometries, with favorable positioning of the interacting charged groups with respect to each other, are likely to be stabilizing, regardless of their location in the protein structure. Our extensive, large-scale analysis finds that the majority of the salt bridges are local in sequence, consistent with the hierarchical model for protein folding (Baldwin & Rose, 1999; Tsai *et al*., 1999).

Results and Discussion

General properties of salt bridges in monomeric proteins

Our dataset includes 36 high-resolution proteins. They are non-homologous structure and sequence-wise. In solution, all are biologically active as monomers. Salt bridge formation is inferred for a pair of oppositely charged residues (Asp or Glu with Arg, Lys or His) if they meet the following criteria: (i) The centroids of the side-chain charged groups in oppositely charged residues lie within 4.0 Å of each other (Barlow & Thornton, 1983); and (ii) at least one pair of Asp or Glu side-chain carboxyl oxygen atoms and side-chain nitrogen atoms of Arg, Lys or His are within a 4.0 Å distance.

Side-chain charged group centroids are computed using the coordinates of only the heavy atoms.

These criteria ensure selection of salt bridges with ''good'' geometries in our database. Using these criteria, we have selected a database of 222 non-equivalent salt bridges from the 36 non-homologous monomeric proteins. We observe that the number of salt bridges increases with the number of residues in proteins (data not shown). Most of the salt bridges are formed between sequentially close residues. This is illustrated in Figure 1, which plots the number of salt bridges against the number of amino acid residues separating the salt-bridging residues. This observation is in agreement with the hierarchical model of protein folding (Baldwin & Rose, 1999; Tsai *et al*., 1999). Furthermore, residues forming salt bridges tend to cluster in helical and strand regions of the Ramachandran map (data not shown). We have next divided the database of 222 salt bridges into different classes according to their locations, i.e. buried or exposed, networked or isolated, and with respect to the presence or absence of hydrogen bonds.

The location of residues forming salt bridges is characterized in terms of the solvent accessible surface areas (ASA) (Lee & Richards, 1971; Tsai & Nussinov, 1997) of their constituent residues, with a probe radius of 1.4 Å. The location of a salt bridge in the protein is estimated by the average ASA of the salt bridge. The average ASA of a salt bridge is average of the ASAs of the two salt-

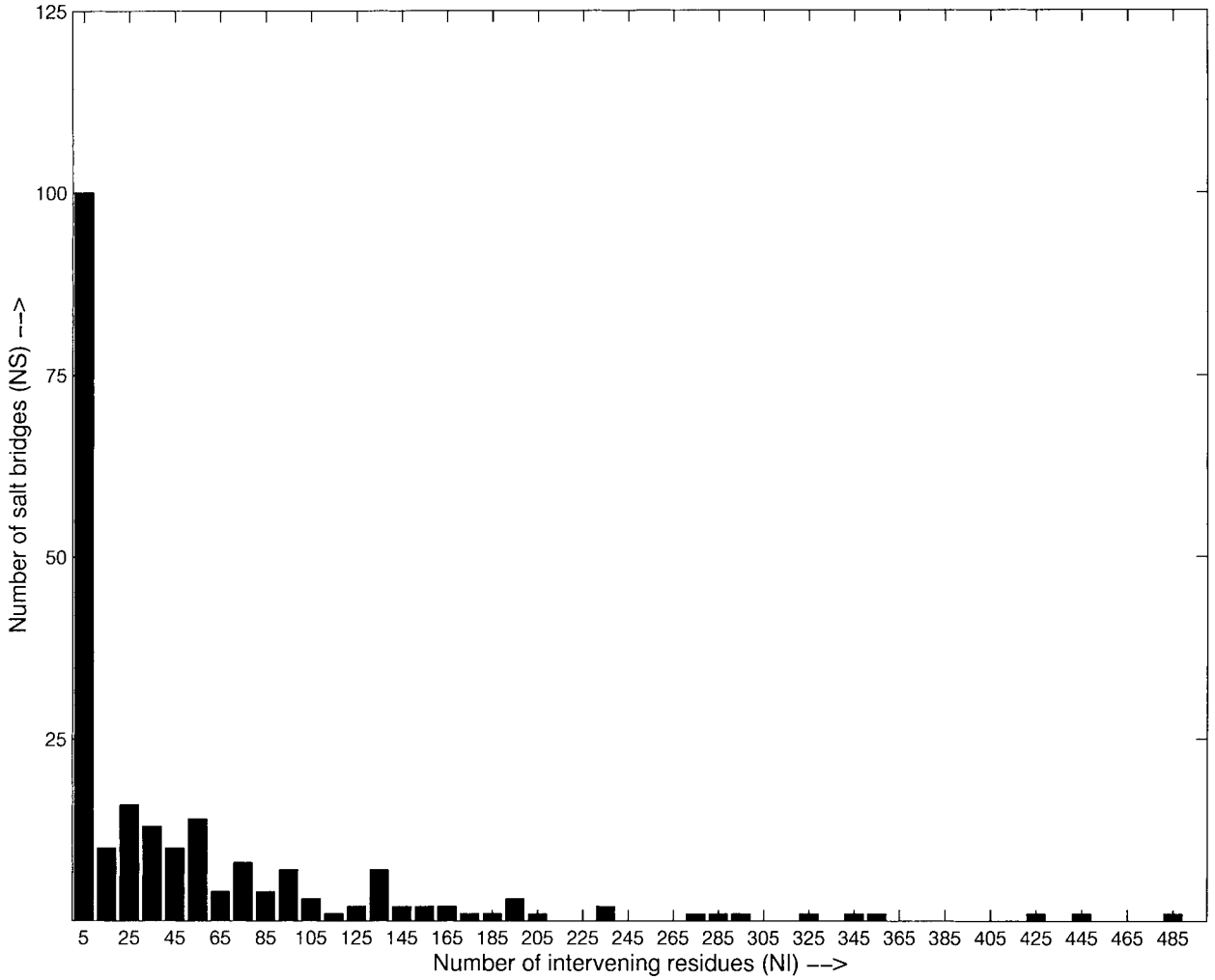

Figure 1. A histogram showing the number of salt bridges with respect to the number of intervening residues. The number of intervening residues (NI, along the *X*-axis) is the number of residues separating the two salt-bridging residues in the amino acid sequence of the proteins. The number of salt bridges (NS) is plotted along the *Y*-axis. Oppositely charged residues sequentially near each other form salt bridges with much greater frequency than residues that are sequentially far apart.

bridging residues. A salt bridge is classified as being buried in the protein core if it has an average ASA of $\leqslant 20\,\%$, otherwise it is classified as being exposed to the solvent. In our dataset, 66 out of the 222 (30 %) salt bridges are buried, with the remainder 156 being exposed. Side-chains of charged amino acids, especially those of Arg and Lys, contain hydrophobic parts. The distribution of the salt bridges with respect to their locations may reflect a competition between the hydrophilic/charged functional groups and the hydrophobic parts of these side-chains. In the dataset, there are six types of residue pairs in the salt bridges: Lys-Asp, Lys-Glu, Arg-Asp, Arg-Glu, His-Asp and His-Glu. All but four salt bridges in our dataset contain either Lys or Arg. A change in proportion test (Kumar & Bansal, 1998) indicates that the decrease in proportions of Lys-Asp and Lys-Glu pairs in buried salt bridges is highly significant. The increase in the proportion of the Arg-Asp pair in buried salt bridges is also highly significant. Hence, buried salt bridges prefer Arg over Lys, while exposed salt bridges prefer Lys over Arg. No such discrimination is observed in the database with respect to the negatively charged residues, Asp and Glu. The above observations are consistent with an earlier analysis of the residue composition in the interior of proteins as compared to that in protein-protein interfaces (Tsai *et al.*, 1997). This analysis, conducted in our laboratory, had shown that a much larger proportion of Arg is buried in the protein interior as compared to Lys. The difference in the proportions of Glu and Asp that are buried in the protein interior is not as large (Tsai *et al.*, 1997).

A salt bridge between two charged residues is considered to be networked if at least one of these charged residues forms additional salt bridge(s) with other charged residue(s) in the protein. Other-

wise, the salt bridge is considered to be isolated. A total of 205 out of the 222 (92%) salt bridges are isolated. The remaining 17 salt bridges are part of four triads and three tetrads salt bridge networks.

The geometry of a salt bridge is characterized in terms of the distance between the centroids of the salt-bridging residue side-chain charged groups, and the angular orientation of these groups with respect to each other. The angular orientation of the side-chain charged groups in the two salt-bridging residues is computed as the angle between two unit vectors. Each unit vector joins a C^{α} atom and a side-chain charged group centroid in a salt-bridging residue. As described above, our criteria ensure good geometries of the salt bridges in our database. Consequently, 191 (86%) salt bridges in our database contain at least one side-chain to side-chain hydrogen bond. A hydrogen-bonded salt bridge is identified by the presence of at least one pair of side-chain charged group atoms, with opposite partial charges, within a 3.5 Å distance.

Continuum electrostatic calculations of salt bridge energetics

Understanding the electrostatic properties of a protein in aqueous solution requires an accurate description of the solute (protein), the solvent (water) and the interaction between them. Continuum methods, based on classical electrostatics, model solute molecules in atomic detail, but treat the solvent in terms of average (bulk) properties. In recent years these methods have been widely used as quantitative tools that provide an accurate description of electrical potentials, pH-dependent properties of proteins and solvation free energies of organic molecules (Honig & Nicholls, 1995). Computations of the electrostatic contributions to free energy change upon salt bridge formation, using continuum electrostatic calculations, have already been performed (Hendsch & Tidor, 1994; Lounnas & Wade, 1997; Xu *et al*., 1997b; Elcock, 1998; Kumar *et al*., 1999; Xiao & Honig, 1999). We have essentially followed the computational method by Hendsch & Tidor (1994). This method calculates the free energy of a salt bridge relative to computer mutations of the salt-bridging residue side-chains to their hydrophobic isosteres. The hydrophobic isosteres are the salt-bridging residue side-chains with their partial atomic charges set to zero. This method has been widely used in the literature (Hendsch & Tidor, 1994; Lounnas & Wade, 1997; Xu *et al*., 1997b; Barril *et al*., 1998; Xiao & Honig, 1999). Predictions made from calculations using this method have also been experimentally verified (Waldburger *et al*., 1995, 1996). The electrostatic contribution to free energy change upon salt bridge formation in a protein can be partitioned into three component terms: (i) $\Delta\Delta G_{dslv}$ represents the sum of the unfavorable desolvation penalties incurred by the individual salt-bridging residues due to the change in their environment from a high dielectric solvent (water) in the unfolded state, to the low dielectric protein interior in the folded state of the protein. (ii) $\Delta\Delta G_{brd}$ represents the favorable bridge energy due to the electrostatic interaction of the side-chain charged groups with each other in the folded state of the protein. (iii) $\Delta\Delta G_{prt}$ represents the electrostatic interaction of the salt-bridging side-chains with the charges in the rest of the protein in the folded state of the protein.

The total electrostatic contribution to the free energy change upon formation of a salt bridge, $\Delta\Delta G_{tot}$, is the sum of the three components:

$$\Delta\Delta G_{tot} = \Delta\Delta G_{dslv} + \Delta\Delta G_{brd} + \Delta\Delta G_{prt}$$

The association energy, $\Delta\Delta G_{assoc}$, takes into account the desolvation of the salt bridge and the electrostatic interaction between the salt-bridging side-chains, but does not consider the electrostatic interaction of the salt bridge with the rest of the protein. Hence, it represents the electrostatic contribution to the free energy change upon salt bridge formation in the absence of charges in the rest of the protein (Hendsch & Tidor, 1994).

While overall the methodologies employed in the present study and in the study by Hendsch & Tidor (1994) are similar, there are a few variations in the actual protocols that are followed. For example, we have used the PARSE parameter set (Sitkoff *et al*., 1994) to assign partial atomic charges. Further, we have added all the hydrogen atoms to the protein. However, these variations do not contribute to any significant differences in the various free energy terms. The Materials and Methods details the similarities and the differences between the Hendsch & Tidor procedure and our protocol.

Observations on all 222 salt bridges

The calculated electrostatic free energies for all 222 salt bridges are presented in the Supplementary Material. On average, salt bridges incur a desolvation penalty $\Delta\Delta G_{dslv}$ of +6.5(±5.5) kcal/mol. This penalty is paid almost entirely by the bridge energy term $\Delta\Delta G_{brd}$ with an average of −6.3(±4.4) kcal/mol. The electrostatic interaction of a salt bridge with the rest of the protein $\Delta\Delta G_{prt}$ is, on average, stabilizing by −3.9(± 4.4) kcal/mol. The association energy $\Delta\Delta G_{assoc}$ averages at −3.6(±2.6) kcal/mol. The profiles of various energy terms in the 222 salt bridges are shown in Figure 2(a). An overwhelming majority of the salt bridges in our database are stabilizing: 190 out of the 222 (85.6%). The remaining 32 (14.4%) salt bridges are destabilizing. The average $\Delta\Delta G_{tot}$ is −3.7(±3.9) kcal/mol. In general, a favorable bridge energy term appears to be the dominant factor in neutralizing the incurred unfavorable desolvation energy penalty. A favorable interaction of the salt-bridging side-chains with the rest of the protein, i.e. the protein energy term, assists the bridge energy term to overcome the desolvation energy

penalty, making the salt bridge stabilizing. Interestingly, the protein energy term $\Delta\Delta G_{prt}$ is destabilizing for 25 out of 222 (11.3 %) salt bridges. However, the average destabilization is only +0.9(±1.3) kcal/mol, with a range of +0.03 to +4.8 kcal/mol. A total of 12 out of the 25 bridges are still stabilizing. The main reason for the remaining 13 salt bridges to be destabilizing is the inability of their respective bridge energy terms to compensate for the desolvation penalties. This trend is consistent with that observed for the other 19 (out of 32) destabilizing salt bridges. Hence, salt bridge stability is largely governed by the desolvation penalty and the bridge energy. The electrostatic interaction of the salt bridge with its protein environment is of secondary importance. Exceptions to this rule are observed for the networked salt bridges.

The energy terms for the 222 salt bridges are plotted against the average ASAs of the salt bridges in Figure 2(b). The desolvation energy penalty decreases substantially with the increase in the average ASA of the bridges. This is consistent with previous studies that indicated an increased desolvation penalty for buried salt bridges (Hendsch & Tidor, 1994; Honig & Hubell, 1984). Here, we investigate further the nature of this relationship between salt bridge burial and the desolvation energy penalty. Figure 2(c) presents the linear regression between $\Delta\Delta G_{dslv}$ and the average ASA, and between $\log(\Delta\Delta G_{dslv})$ and the average ASA. The square of the linear regression coefficient yields a slightly better regression between $\log(\Delta\Delta G_{dslv})$ and the average ASA. The root-mean-squared deviation (r.m.s.d.) in this case is 0.52. Hence, the data appear more consistent with an exponential relationship between the desolvation penalty and the average ASA.

This relationship can be written as follows:

$$\log(\Delta\Delta G_{dslv}) = -0.0465018 ASA_{av} + 2.89433$$

where $\Delta\Delta G_{dslv}$ is in kcal/mol and ASA_{av} is in %.

The high linear correlation coefficient ($r^2 = 0.69$) and the low r.m.s.d., suggest that the location of the salt bridge in the protein may largely determine its desolvation penalty. Figure 2(b) shows that the desolvation energy penalty tends to shoot up for salt bridges with an average ASA below 20 %, i.e. for buried salt bridges.

Figure 2(b) also illustrates the dependence of the bridge and protein energy terms on the average ASA of the salt bridges. In general, buried salt bridges tend to have stronger bridge and protein energy terms. However, the trends for the bridge and protein energy terms are not as clear cut as in the case of the desolvation energy penalty. The dependence of the bridge and protein energy terms on the average ASA illustrates the effect of the local environment around the salt bridge on the interaction between the side-chains in the salt bridge, and the interaction of the salt bridge with the rest of the protein. Buried salt bridges are likely to be surrounded by a more hydrophobic environment. Such an environment will have a low effective dielectric constant. Hence, electrostatic interactions both between the bridge side-chains, and with neighboring charges are not solvent screened. On the other hand, in exposed salt bridges, the local environment is likely to be more polar and hence will have a higher effective dielectric constant. The high effective dielectric constant medium can effectively screen such interactions. A weak trend is also observed between the total free energy of a salt bridge and its average ASA. Buried salt bridges tend to be more stabilizing than exposed ones. However, there is a large scatter in the data. The association energy for the salt bridges $\Delta\Delta G_{assoc}$ is favorable for the 222 salt bridges (see Figure 2(a) and (b)), and does not vary much with the average ASAs.

Below we compare and analyze salt bridge energetics in various categories of the dataset.

Stabilizing and destabilizing salt bridges

A total of 190 (85.6 %) out of the 222 salt bridges in our database are stabilizing. Table 1 presents the average values for the energy terms for stabilizing

Table 1. Average energy terms in various salt bridge categories

Salt bridge class	$\Delta\Delta G_{dslv}$ (kcal/mol)	$\Delta\Delta G_{brd}$ (kcal/mol)	$\Delta\Delta G_{prt}$ (kcal/mol)	$\Delta\Delta G_{tot}$ (kcal/mol)	$\Delta\Delta G_{assoc}$ (kcal/mol)
All	+6.54 ± 5.48	−6.34 ± 4.38	−3.86 ± 4.35	−3.66 ± 3.86	−3.64 ± 2.63
Stable	+6.39 ± 5.38	−6.60 ± 4.32	−4.40 ± 4.37	−4.61 ± 3.21	−3.88 ± 2.67
Destable	+7.44 ± 6.06	−4.76 ± 4.45	−0.69 ± 2.53	+1.99 ± 2.17	−2.22 ± 1.85
Buried	+12.89 ± 5.59	−10.17 ± 4.58	−7.26 ± 5.46	−4.53 ± 5.13	−4.37 ± 2.66
Exposed	+3.85 ± 2.28	−4.71 ± 3.11	−2.43 ± 2.75	−3.29 ± 3.11	−3.33 ± 2.56
Isolated	+6.37 ± 5.47	−6.30 ± 4.46	−3.56 ± 4.21	−3.48 ± 3.92	−3.66 ± 2.70
Networked	+8.58 ± 5.17	−6.82 ± 3.37	−7.57 ± 4.52	−5.81 ± 2.10	−3.40 ± 1.64
H-bonded	+6.67 ± 5.50	−6.64 ± 4.48	−3.82 ± 4.15	−3.79 ± 3.89	−3.83 ± 2.68
No H-bonds	+5.74 ± 5.34	−4.46 ± 3.19	−4.14 ± 5.51	−2.87 ± 3.60	−2.45 ± 1.99

All, whole dataset of 222 salt bridges; Stable, 190 salt bridges with $\Delta\Delta G_{tot} < 0$ kcal/mol; Destable, 32 salt bridges with $\Delta\Delta G_{tot} > 0$ kcal/mol; Buried, 66 salt bridges with average ASA of $\leqslant 20$ %; Exposed, 156 salt bridges with average ASA of >20 %; Isolated, 205 salt bridges that do not form part of salt bridge networks; Networked, 17 salt bridges that participate in salt bridge networks; H-bonded, 191 salt bridges containing at least one hydrogen bond between side-chain charged groups; and No H-bonds, 31 salt bridges that do not contain any hydrogen bond between their side-chain charged groups.

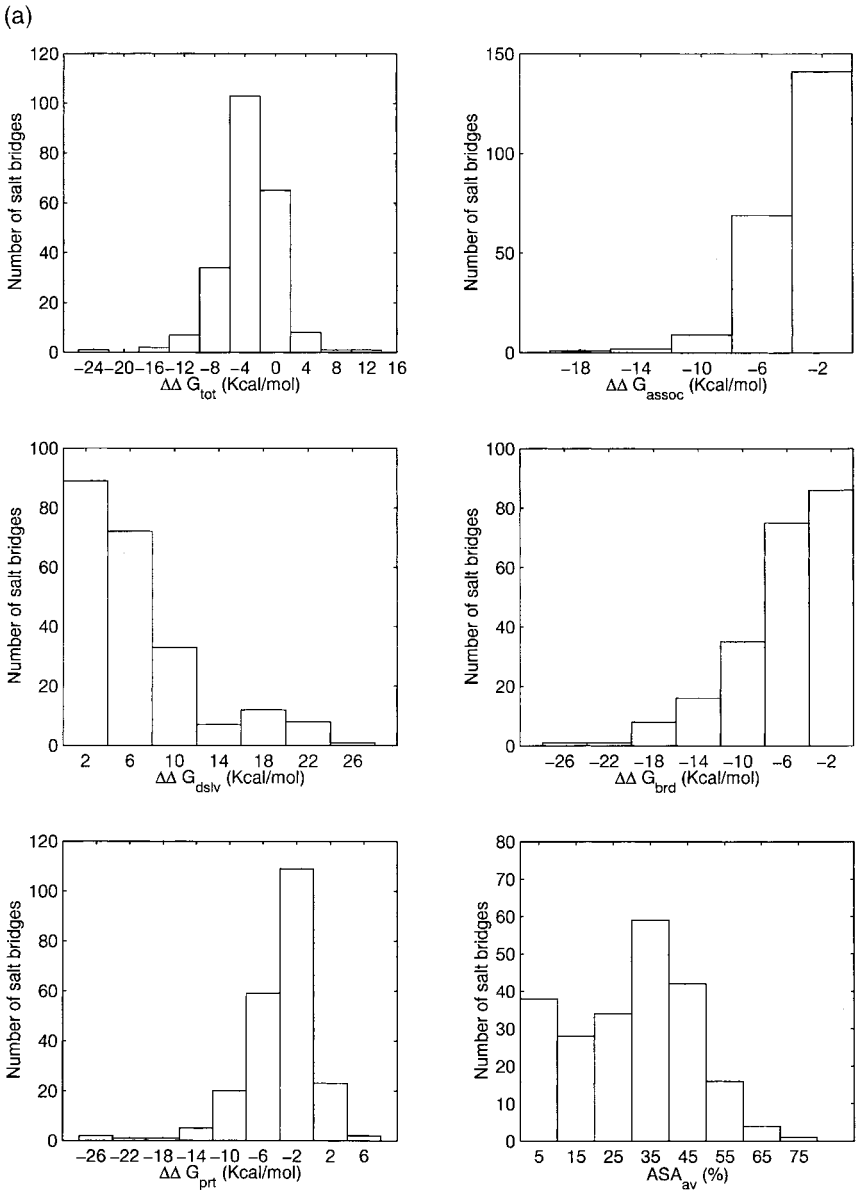

Figure 2 (*legend shown on page 1248*)

and destabilizing salt bridges. In the destabilizing salt bridges, the unfavorable desolvation energy is approximately 1 kcal/mol higher than that in the stabilizing bridges. The bridge energy term is weaker by about 2 kcal/mol and the protein energy term is reduced by about 4 kcal/mol (Table 1). These three factors combine to render these salt bridges to be, on average, destabilizing by 2 kcal/mol. As noted above, 13 out of the 32 destabilizing salt bridges contain a destabilizing protein term as well.

Table 2A shows that 55 out of the 190 (29 %) stabilizing salt bridges are buried, 135 (71 %) are exposed. These proportions are very similar to those for all 222 salt bridges; 34 % ($11 \times 100/32$) of the destabilizing salt bridges are buried. This indicates only a marginal tendency for a larger proportion of the destabilizing salt bridges to be buried. Based on previous work (Hendsch & Tidor, 1994; Waldburger *et al.*, 1995, 1996) we would have expected to observe a stronger tendency for the destabilizing salt bridges to be buried. However, burial is not the only criteria for salt bridge stability. Our results indicate that the geometry of a salt bridge should also be considered, since the desolvation penalty is mostly compensated by the bridge energy term. In their continuum electrostatic analysis, Hendsch & Tidor (1994) have used salt bridges from experimentally well-studied proteins. Unlike in our studies here, no geometrical criteria were considered in the selection and assessment of their dataset of salt bridges. Upon examination of the geometries of their salt bridges, we find that the side-chain centroid distances in their

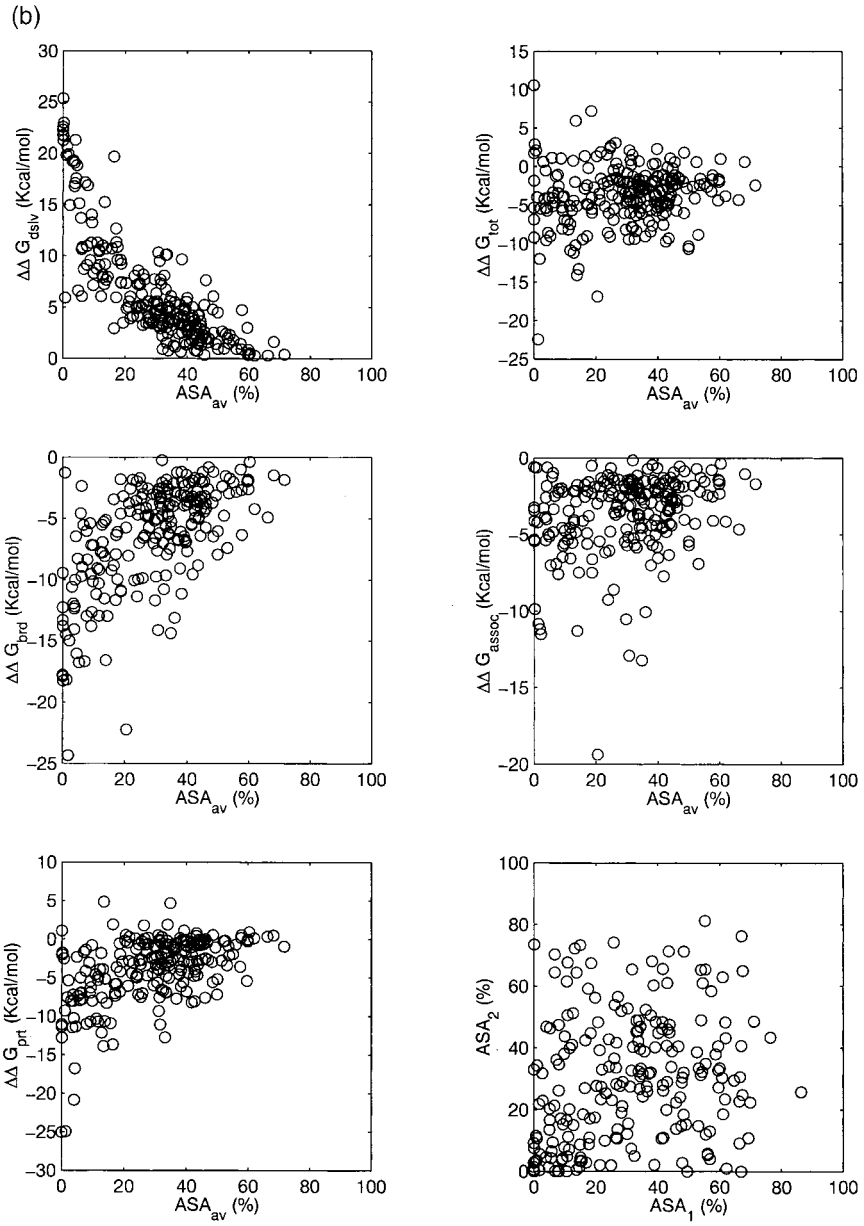

Figure 2 (*legend shown on page 1248*)

salt bridges range between 3.1 Å and 5.8 Å, with the majority being greater than 4.0 Å. Hence, most of the salt bridges in their dataset, are not within the 4.0 Å range that we allow. In general, salt bridges with side-chains far apart have weaker bridge energy terms as compared to those with closer side-chains. Weak bridge energy terms are unable to compensate for the desolvation penalties, rendering most of the salt bridges in the Hendsch & Tidor dataset destabilizing. We note that our stricter geometrical criteria in identifying and selecting salt bridges, reject bridges with poor interaction between the charged groups of the side-chains. The procedure to which we adhere throughout this work is likely to lead to filtering out salt bridges with poor geometries from our dataset.

Buried and exposed salt bridges

Buried salt bridges in protein structures have often been thought to be destabilizing (Honig & Hubell, 1984; Dao-pin, 1991; Hendsch & Tidor, 1994; Waldburger *et al.*, 1995). Exceptions have been noted by Lounnas & Wade (1997) for the cytochrome *P*-450 cam. Table 1 shows that buried salt bridges indeed pay a high desolvation penalty. The average $\Delta\Delta G_{dslv}$ for the 66 buried salt bridges is +12.9(±5.6) kcal/mol. This large desolvation penalty is offset by the large bridge and protein

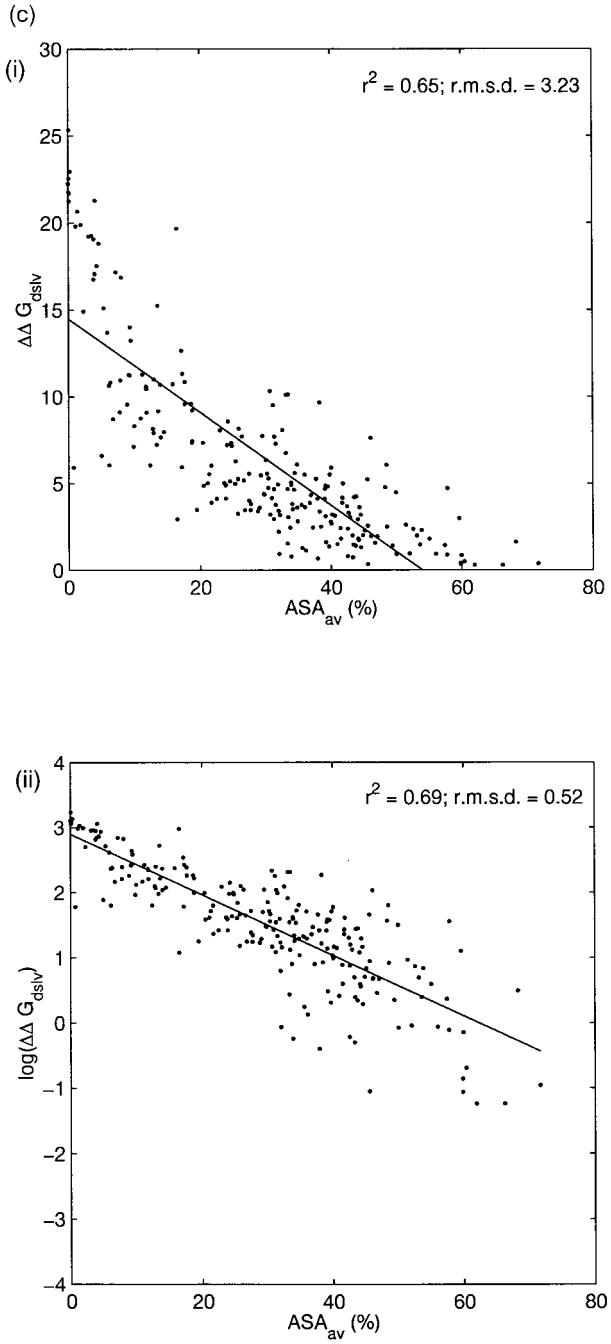

Figure 2. Energetic analysis of 222 salt bridges. (a) Histograms showing profiles for various energy terms for the 222 salt bridges and for the average accessible surface area (ASA) for the salt bridges. Quantities marked by energy terms along the *X*-axes of the histograms are explained in the text. The *Y*-axis in each histogram indicates the number of salt bridges. The *X*-axis for the histogram in the lower-most right-hand diagram in the panel indicates average ASA of the salt-bridging residues, instead of an energy term. Most of the salt bridges in our dataset are stabilizing. The protein energy term can be destabilizing in some cases. The association energy, $\Delta\Delta G_{assoc}$, is always stabilizing for the salt bridges. (b) The variation of the energy terms (*Y*-axis) with respect to the average ASA (*X*-axis) of the salt bridges. The lower-most right diagram plots the accessible surface areas (ASA) for the residues in the salt bridges. The overall stability of the salt bridges, $\Delta\Delta G_{tot}$, shows a weak dependence on location of the salt bridges in the protein. $\Delta\Delta G_{brd}$ and $\Delta\Delta G_{prt}$ tend to be less stabilizing as the average ASA increases. Thus, these terms tend to have greater stabilization for buried salt bridges than exposed bridges. $\Delta\Delta G_{dslv}$ tends to decrease with average ASA, i.e. buried salt bridges pay higher desolvation penalties than the exposed salt bridges. $\Delta\Delta G_{dslv}$ shows the strongest trend with average ASA of the salt bridges. (c) Two possible relationships between $\Delta\Delta G_{dslv}$ and the average ASA that appear to be most consistent with the data. In each plot, (·) symbols indicate actual data points and a best fit line is shown for the variables on the *X* and *Y*-axes. (i) Linear relationship between $\Delta\Delta G_{dslv}$ (*Y*-axis) and ASA_{av} (*X*-axis). The square of the correlation coefficient (r^2) is 0.65 and the root-mean-square deviation (r.m.s.d.) of the observed points from the best fit line is 3.23. (ii) Linear relationship between $\log(\Delta\Delta G_{dslv})$ (*Y*-axis) and ASA_{av} (*X*-axis). The square of the correlation coefficient (r^2) is 0.69 and the r.m.s.d. of the observed points from the best fit line is 0.52. The logarithmic relationship is more consistent with the data.

Table 2. Salt bridge distributions in monomeric proteins.

A. *Buried and exposed salt bridges in various salt bridge categories*			
Salt bridge class	Buried	Exposed	Total
All	66 (29.7%)	156 (70.3%)	222
Stable	55 (28.9%)	135 (71.1%)	190
Destable	11 (34.4%)	21 (65.6%)	32
Isolated	60 (29.3%)	145 (70.7%)	205
Networked	6 (35.3%)	11 (64.7%)	17
H-bonded	59 (30.9%)	132 (69.1%)	191
No H-bonds	7 (22.6%)	24 (77.4%)	31
B. *Stable and destable salt bridges in various salt bridge categories*			
Salt bridge class	Stable	Destable	Total
All	190 (85.6%)	32 (14.4%)	222
Buried	55 (83.3%)	11 (16.7%)	66
Exposed	135 (86.5%)	21 (13.5%)	156
Isolated	173 (84.4%)	32 (15.6%)	205
Networked	17 (100.0%)	0 (0.0%)	17
H-bonded	166 (86.9%)	25 (13.1%)	191
No H-bonds	24 (77.4%)	7 (22.6%)	31

The various salt bridge classes are explained in the legend to Table 1. Numbers in parentheses indicate percentages, and those outside indicate the number of salt bridges. In each row the percentages add up to 100%.

energy terms. The average $\Delta\Delta G_{brd}$ for the buried salt bridges is $-10.2(\pm4.6)$ kcal/mol and the average $\Delta\Delta G_{prt}$ is $-7.3(\pm5.5)$ kcal/mol. This makes the buried salt bridges in our database mostly stabilizing, with the average $\Delta\Delta G_{tot}$ being $-4.5(\pm5.1)$ kcal/mol (Table 1). Large standard deviations over the mean values indicate a wide scatter in the data, as seen in Figure 2(b). On average, exposed salt bridges pay substantially smaller desolvation penalties. The average $\Delta\Delta G_{dslv}$ for the 156 exposed salt bridges is $+3.8(\pm2.3)$ kcal/mol. This small desolvation penalty is overcome by the correspondingly smaller bridge and protein energy terms. The average $\Delta\Delta G_{brd}$ for the exposed salt bridges is $-4.7(\pm3.1)$ kcal/mol and the average $\Delta\Delta G_{prt}$ is $-2.4(\pm2.75)$ kcal/mol. This makes the exposed salt bridges in our database largely stabilizing, with the average $\Delta\Delta G_{tot}$ $-3.3(\pm3.1)$ kcal/mol. Taken together, these results indicate that in our dataset buried salt bridges are slightly more stabilizing than exposed ones. The average difference in stability is $\sim$1.2 kcal/mol. However, this result should be treated with caution due to a large scatter in the data (Table 1 and Figure 2(b)). The association energies of buried and exposed salt bridges show similar trends. The average $\Delta\Delta G_{assoc}$ for buried salt bridges is $-4.4(\pm2.7)$ kcal/mol, while that for an exposed salt bridge is $-3.3(\pm2.6)$ kcal/mol.

Our database contains 17 networked salt bridges. Six of these are buried (Table 2A). Based on uniform distribution of the networked salt bridges over the whole average ASA range, we would expect five ($66 \times 17/222$) networked salt bridges to be buried. Hence, networking is not responsible for the larger magnitude of the protein energy term for the buried salt bridges. There can be two alternative reasons for the above observations. First, the electrostatic interactions between salt-bridging side-chains and their protein environment face reduced solvent screening in the interior of the protein. This argument is similar for both protein and bridge energy terms and has been already noted above. Second, charges present in the neighborhood of buried salt bridges may have favorable electrostatic interactions with the buried bridges.

Isolated and networked salt bridges

As mentioned earlier, our database has only 17 (8%) networked salt bridges. The remaining 205 are isolated salt bridges. Table 1 shows that isolated and networked salt bridges pay similar desolvation penalties, which are almost neutralized by similar bridge energy terms. However, the average protein energy term of the networked salt bridges is more than double that of the isolated salt bridges. Networked salt bridges have an average $\Delta\Delta G_{prt}$ of $-7.6(\pm4.5)$ kcal/mol, while isolated salt bridges have an average $\Delta\Delta G_{prt}$ of $-3.6(\pm4.2)$ kcal/mol. This increase in the protein energy term for the networked salt bridges is responsible for their greater electrostatic stability. The average $\Delta\Delta G_{tot}$ for the networked salt bridges is $-5.8(\pm2.1)$ kcal/mol. The average $\Delta\Delta G_{tot}$ for the isolated salt bridges is $-3.5(\pm3.9)$ kcal/mol. In the networked salt bridges the protein energy term is similar in magnitude to the bridge energy term. Thus, here the electrostatic interaction of the salt bridge with its protein neighborhood is no longer of secondary importance.

Consistently, we have also observed that the salt bridges in glutamate dehydrogenase (GDH) from the hyperthermophilic archaeon *Pyrococcus furiosus* have larger stabilities than those in glutamate dehydrogenase from the mesophile *Clostridium symbiosum* (Kumar *et al*., 1999). The thermophilic GDH contains a larger number of salt bridges, and most of these are networked. Salt bridges in the thermophilic GDH also have a large protein energy term, similar in magnitude to the bridge energy

term (Kumar *et al*., 1999). Thus, the increased frequency of salt bridges and their networks can enhance the stability of a protein. Recently, deBakker *et al*. (1999) have also observed similar trends in a molecular dynamics study of *Sulfolobus acidocaldarius* Sac7d protein. Recent electrostatic calculations by Xiao & Honig (1999) are consistent with these arguments.

Table 2B shows that all the 17 networked salt bridges are stabilizing. In comparison, 173 (84%) of the isolated salt bridges are stabilizing. Since the number of networked salt bridges in our dataset is small, we cannot draw a conclusion that all networked salt bridges in proteins are stabilizing. Nevertheless, it is clear that the majority of the networked salt bridges are stabilizing.

Hydrogen bonded and non-hydrogen bonded salt bridges

Our present study treats both hydrogen bonded and non-hydrogen bonded salt bridges as purely electrostatic interactions. We do not include a hydrogen bonding energy term in our model. The distinction between the salt bridges that contain side-chain to side-chain hydrogen bonds and those which do not contain such hydrogen bonds is based solely on geometrical considerations. Hence, the hydrogen bonded salt bridges can also be considered as short range salt bridges.

A total of 191 out of 222 (86%) salt bridges in our dataset contain at least one hydrogen bond between their side-chains. A hydrogen bond is inferred if a pair of side-chain nitrogen and oxygen atoms in the two residues is within a 3.5 Å distance. The remaining 31 salt bridges do not contain any hydrogen bond. On average, the hydrogen bonded salt bridges are more stabilizing as compared to the non-hydrogen bonded salt bridges. The hydrogen bonded salt bridges have average $\Delta\Delta G_{tot}$ of $-3.8(\pm3.9)$ kcal/mol, whereas average $\Delta\Delta G_{tot}$ for the non-hydrogen bonded salt bridges is $-2.9(\pm3.6)$ kcal/mol. Charged groups forming a salt bridge can interact more effectively if they are hydrogen bonded because the oppositely charged atoms are closer to one another. Consequently, hydrogen bonded salt bridges have stronger bridge energy terms. The average $\Delta\Delta G_{brd}$ for the hydrogen bonded salt bridges is $-6.6(\pm4.5)$ kcal/mol, while that for the non-hydrogen bonded salt bridges is $-4.5(\pm3.2)$ kcal/mol.

The distributions of the hydrogen bonded salt bridges are as expected from the whole database. A total of 59 (31%) of the hydrogen bonded salt bridges are buried and 132 (69%) are exposed. Table 2B shows that 166 out of the 191 (87%) hydrogen bonded salt bridges are stabilizing and the remaining 25 are destabilizing. On the other hand, the non-hydrogen bonded salt bridges deviate from the expected distributions. Though large in proportions, these deviations are not statistically significant. Seven (23%) non-hydrogen bonded salt bridges are buried and the remaining 24 are exposed (Table 2A). Based on a uniform distribution of the non-hydrogen bonded salt bridges with respect to their location in the protein, we would expect nine non-hydrogen bonded salt bridges to be buried and the remaining 22 to be exposed. A total of 24 (77%) non-hydrogen bonded salt bridges are stabilizing and seven are destabilizing. Again, if the distribution of non-hydrogen bonded salt bridges were uniform with respect to stability, we would expect 27 non-hydrogen bonded salt bridges to be stabilizing and four to be destabilizing. Thus, non-hydrogen bonded salt bridges contain a greater than expected proportion of destabilizing salt bridges. Atoms with opposite partial charges in the side-chain charged groups of the non-hydrogen bonded salt bridges are farther apart as compared to those in the hydrogen bonded salt bridges. Hence, an increased proportion of the destabilizing salt bridges can be rationalized. We note that non-hydrogen bonded salt bridges still have at least one pair of atoms with opposite partial charges within a 4.0 Å distance. A larger proportion of salt bridges with atoms bearing opposite partial charges farther apart (>4.0 Å), will be destabilizing. Such residue pairs are eliminated from our database.

Interesting individual salt bridges

Above, we have provided a description of the average properties of the salt bridges in their different categories. Here, we pick specific interesting salt bridges. We discuss three examples: two salt bridges are highly buried in the protein core. The electrostatic interaction between their respective salt-bridging charged groups, as well as their surroundings differ, making one salt bridge the most stabilizing and the other the most destabilizing in our dataset. The third salt bridge pays almost no desolvation cost. This salt bridge resides on the surface, almost completely exposed to the solvent. The electrostatic interactions in this case are strongly screened by water. The net result is a stabilizing salt bridge. These salt bridges are shown in Figure 3.

The most stabilizing salt bridge

The most stabilizing salt bridge in our database is formed by residues Glu27 and Arg387 in the human salivary α-amylase (PDB code: 1smd). The calculated $\Delta\Delta G_{tot}$ for this salt bridge is -22.4 kcal/mol. This is an isolated and highly buried bridge, with an average ASA of 1.37%. Due to its highly buried nature, this salt bridge pays a high desolvation penalty, $\Delta\Delta G_{dslv}$, of $+20.7$ kcal/mol. However, this desolvation penalty is easily paid off by equally high bridge and protein energy terms. The calculated $\Delta\Delta G_{brd}$ for this salt bridge is -18.2 kcal/mol and $\Delta\Delta G_{prt}$ is -24.9 kcal/mol. The charged groups in Glu27 and Arg387 interact

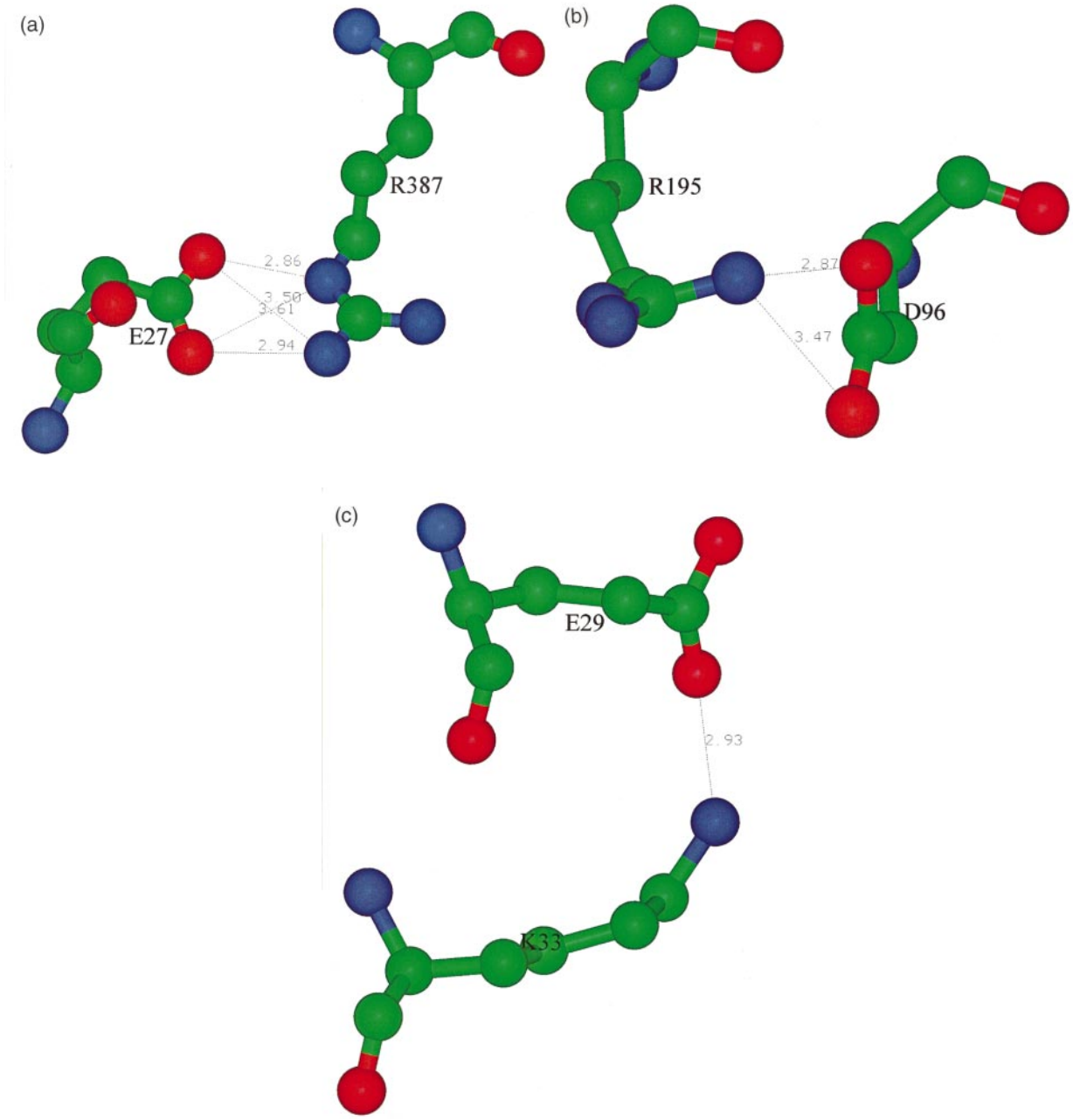

Figure 3. Interesting salt bridges in our database. (a) The most stabilizing salt bridge in our database is formed by E27 and R387 in human salivary α-amylase (PDB code 1smd). The salt bridge has excellent geometry. Three hydrogen bonds (two of them strong) are formed between side-chain charged groups. This salt bridge is buried in the protein core and pays high desolvation penalty. However, this penalty is easily paid off by large bridge and protein terms. (b) The most destabilizing salt bridge in our database is formed by D96 and R195 also in human salivary α-amylase (PDB code 1smd). The salt bridge has very good geometry. It contains a bifurcated hydrogen bond and, hence, has large bridge energy. This salt bridge is also buried in the protein core and pays high desolvation penalty. However, this penalty is not paid off by the bridge energy term. The protein energy term is destabilizing for this salt bridge. (c) A salt bridge that pays almost no desolvation penalty. This salt bridge is formed by Glu29 and Lys33 in *Streptococcal* protein G (PDB code 1igd). It is almost completely exposed to the solvent and has minimal interaction with the rest of the protein. The protein energy term is also negligible. The salt bridge has good geometry and contains a strong hydrogen bond. This bridging electrostatic interaction is strongly screened by the solvent. In spite of this, the salt bridge is stabilizing.

strongly with each other as well as with their environment. The side-chain charged group centroids are 3.71 Å apart. The angle between the vectors that join the C^{α} atoms and the side-chain charged group centroids is 46.3°, resulting in a very good bridge geometry. The side-chain carboxyl oxygen atoms in Glu27 form three hydrogen bonds (two of which are strong) with the side-

chain nitrogen atoms in the guanidium group of Arg387 (Figure 3(a)). A few atoms with net partial charges are present within 4 Å of this salt bridge. Guanidium group nitrogens N^{ε} and $N^{\eta 2}$ of Arg30 are close to the Glu27 side-chain carboxyl oxygen $O^{\varepsilon 1}$, and the backbone carboxyl oxygen atom of Thr376 is close to the guanidium nitrogen atoms N^{ε} and $N^{\eta 1}$ of Arg387. The association energy for this bridge, $\Delta\Delta G_{assoc}$, is also high (−10.8 kcal/mol). Based on the above observations, we would expect the stability of the protein to decrease if this salt bridge is disrupted.

The most destabilizing salt bridge

The most destabilizing salt bridge in our database is again from the human salivary α-amylase (PDB code: 1smd). This salt bridge is formed between residues Asp96 and Arg195. The calculated $\Delta\Delta G_{tot}$ for this salt bridge is +10.6 kcal/mol. This salt bridge is also isolated and extremely buried with average ASA 0.04%. Due to its burial, it also pays a high desolvation penalty, $\Delta\Delta G_{dslv}$, of +21.8 kcal/mol. However, this penalty is not recovered by the bridge energy term. As in the previous example, this salt bridge is also hydrogen bonded, but it does not have as good a geometry as in the previous case. The side-chain charged group centroids are 3.98 Å apart. The angle between the vectors that join the C^{α} atoms and the side-chain charged group centroids of Asp96 and Arg195 is 165.7°. Nevertheless, the side-chain carboxyl oxygen atoms $O^{\delta 1}$ and $O^{\delta 2}$ in Asp96 form a bifurcated hydrogen bond with the side-chain nitrogen atom $N^{\eta 1}$ in the guanidium group of Arg195 (Figure 3(b)), resulting in a highly favorable bridge energy term, $\Delta\Delta G_{brd}$ of −12.3 kcal/mol. Still, it leaves a large difference of 9.5 kcal to be overcome by the protein energy term. This would require a strong favorable electrostatic interaction between the salt bridge and the rest of the protein. Instead, the interaction of the charged groups of the bridge with the rest of the protein is slightly destabilizing ($\Delta\Delta G_{prt} = +1.1$ kcal/mol). Several atoms with partial charges are within 4 Å distance from this bridge. The backbone nitrogen atom of Ala97 is near the side-chain $O^{\delta 1}$ atom of Asp96. The $O^{\delta 1}$ atom of Asp197, and the $O^{\varepsilon 1}$ and $O^{\varepsilon 2}$ atoms of Glu233 surround the guanidium group nitrogen atoms $N^{\eta 1}$ and $N^{\eta 2}$ of Arg195. The presence of a large number of charges can also have an adverse effect of causing repulsions and increasing the local effective dielectric of the surroundings. The association energy, $\Delta\Delta G_{assoc}$, is −3.2 kcal/mol. One would expect the stability of the protein to increase if this salt bridge is disrupted.

The above examples illustrate two extremes of salt bridges buried deep in the protein core, with practically almost no access of water. Both bridges pay very high desolvation energy costs. However, the substantially different strengths of the interactions, determined by the local positioning of the residues in the salt bridges and those around them, produce opposite results.

A salt bridge that pays almost no desolvation cost

The salt bridge formed by Glu29 and Lys33 in IgG-binding protein domain of *Streptococcal* protein G (PDB code: 1igd) pays a very small desolvation cost ($\Delta\Delta G_{dslv} = +0.3$ kcal/mol). This salt bridge is shown in Figure 3(c). This salt bridge is highly exposed with average ASA of 61.9%. Hence, there is not much change in the surroundings of its charged groups from the unfolded to the folded state of the protein. The salt bridge is stabilizing, with calculated $\Delta\Delta G_{tot}$ of −3.8 kcal/mol. The small desolvation penalty, and even smaller unfavorable protein energy term ($\Delta\Delta G_{prt} = +0.1$ kcal/mol) are easily overcome by the bridge energy term ($\Delta\Delta G_{brd} = -4.2$ kcal/mol). This salt bridge is isolated and contains a hydrogen bond. The side-chain charged group centroids are 3.75 Å apart. The angle between the vectors that join the C^{α} atoms and the side-chain charged group centroids in Glu29 and Lys33 is 155.5°. A strong hydrogen bond is formed between the $O^{\varepsilon 1}$ atom of Glu29 and the N^{ζ} atom of Lys33. This indicates that the salt bridge has a reasonably good geometry and the electrostatic interaction between the charged groups of the side-chains is strong enough. However, this interaction is screened by the solvent. The salt bridge has only a minimal electrostatic interaction with the charges in the rest of the protein. The association energy, $\Delta\Delta G_{asssoc}$, is −4.1 kcal/mol, which is very close to $\Delta\Delta G_{tot}$.

Conclusions

Salt bridges can be stabilizing or destabilizing to the protein structure depending on their geometry, location in the protein, electrostatic interaction between salt-bridging side-chains with each other, and that between the salt bridge and its surroundings. Most of the salt bridges in our dataset are stabilizing, irrespective of whether they are buried or exposed, isolated or networked, hydrogen bonded or not. For most salt bridges, the desolvation cost for bridge formation is paid off primarily by the electrostatic interaction of the salt-bridging residues with each other. The interaction of the salt bridge with the rest of the protein is of secondary importance. However, in the case of the networked salt bridges, both types of interactions have similar magnitudes. A less polar environment of a buried salt bridge, make it pay a higher desolvation energy penalty. However, it also facilitates stronger electrostatic interactions of the salt bridge side-chains with each other and with the charges around them.

The geometrical positioning of the interacting side-chains in the salt bridges with respect to each other, is a very important determinant of salt bridge stability. Salt bridges with good geometries

usually have better electrostatic interactions and are more likely to be stabilizing. On the other hand, our studies indicate that a larger proportion of salt bridges with poor geometries will be destabilizing.

The availability of a dataset of salt bridges derived from a database of structurally and sequence non-redundant set of monomeric proteins, has enabled an examination of the sequence separation between the salt-bridging residues. We find that the sequential distance between two residues which form a bridge is short. This higher occurrence of sequentially short-range over long-range bridges suggests that salt bridge formation is a local phenomenon, consistent with the hierarchical model for protein folding (Baldwin & Rose, 1999; Tsai *et al*., 1999).

Materials and Methods

Database composition

We have selected 222 non-equivalent salt bridges from a set of 36 monomeric proteins. These 36 proteins are non-homologous in sequence (sequence identity is less than 20 %) as well as in structure (determined by a sequence order independent structure comparison technique; Tsai *et al*., 1996). Every protein contains at least 50 residues. The 3D structures of these proteins have been solved to high resolution (1.6 Å or better) by X-ray crystallography and are available in the protein data bank (PDB) (Bernstein *et al*., 1977). Furthermore, the biologically active form of each of these proteins is monomeric as indicated by the PDB file headers and pointers to other databases in the PDB3D browser. The PDB identity codes of these 36 protein are 135l, 153l, 1ads, 1aky, 1akz, 1amm, 1aop, 1arb, 1aru, 1bfg, 1bvd, 1cex, 1cyo, 1dim, 1edg, 1fmk, 1hmr, 1igd, 1mla, 1orc, 1phc, 1ptx, 1rcf, 1rie, 1rro, 1ruv, 1smd, 1tca, 1yge, 1yna, 2ayh, 2dri, 2end, 2eng, 2phy and 3pte.

The salt bridge dataset is divided into several categories based on geometry, location in the protein and networking. The statistical significance of changes in the numbers of salt bridges in these classes of the dataset is determined by a change in proportion test (Kumar & Bansal, 1998).

Computation of the electrostatic free energies of salt bridges

The electrostatic contribution to free energy change upon salt bridge formation is calculated relative to a mutation of its salt-bridging side-chains to their hydrophobic isosteres. Hydrophobic isosteres are identical with the charged residue side-chains, with the exception that their partial atomic charges are set to zero. In each case, all hydrogen atoms are added, the polypeptide chains are capped, and the protonation state of all charged residues at pH 7.0 are defined using the BIOPOLYMER module of INSIGHTII release 98.0 from Molecular Simulations, Inc. Continuum electrostatic calculations are performed with the DELPHI package developed by Honig and co-workers (Gilson *et al*., 1985, 1988; Gilson & Honig, 1987, 1988; Sharp & Honig, 1990; Honig *et al*., 1993) under INSIGHTII release 98.0. The PARSE3 set of partial atomic charges and atomic radii (Sitkoff *et al*., 1994) is used. The PARSE3 set allows reproduction of the experimental data for a wide range of small organic molecules and ions, representing side-chains of amino acids (Radzicka & Wolfenden, 1988). Recently, Hendsch *et al*. (1998) have compared the parameter dependence of continuum electrostatic calculations. They concluded that the CHARMM and PARSE parameter sets yield similar results. Our calculations are in good agreement with those by Hendsch & Tidor (1994). On a randomly selected sample of five salt bridges from their data set, we found excellent correlations for all the energy terms, namely, $\Delta\Delta G_{dslv}$ (linear correlation coefficient, $r = 0.891$), $\Delta\Delta G_{brd}$ ($r = 0.973$), $\Delta\Delta G_{prt}$ ($r = 0.994$) and $\Delta\Delta G_{tot}$ ($r = 0.744$), between our results and those reported by Hendsch & Tidor (1994).

The solvent probe radius used to define the molecular surface is 1.4 Å. The dielectric constant of the solute (the protein molecule) is 4.0 and that of the solvent is 80.0. The ionic strength is 0.0 M, since the current implementation of DELPHI correctly computes the reaction field energies only at zero ionic strength (DELPHI manual). Reaction field energy yields an accurate estimate of the electrostatic solvation energy (DELPHI manual). There is no appreciable effect of the ionic strength on the final values (Hendsch & Tidor, 1994). The Poisson equation is solved using the iterative finite difference method (Gilson *et al*., 1988; Gilson & Honig, 1988; Sharp & Honig, 1990) on a 3D grid with a step of 0.833 Å per grid point, with an energy convergence criterion of 1×10^{-6} kT (kT are the units of energy in DELPHI outputs, k is Boltzmann's constant and T is absolute temperature).

In each calculation, initially the molecule occupies 25-50 % of the grid (depending on the size of the molecule) and the Debye-Huckel (Full Coulombic) boundary conditions are applied (Klapper *et al*., 1986). The resulting grid of this rough calculation is used as a boundary condition for a focused calculation in which the molecule occupies 95 % of the grid. The results of the focused calculations are presented here. DELPHI outputs the energy values in units of kT, where k is the Boltzmann constant and T is absolute temperature. These values are multiplied by a conversion factor of 0.592 to obtain the results in units of kilo calories per mol (kcal/mol) at room temperature (25 °C).

Acknowledgments

We thank Drs Buyong Ma, Chung jung Tsai and Neeti Sinha for helpful discussions. Dr Jacob Maizel is thanked for encouragement to undertake this project. We are also indebted to two anonymous referees for their constructive criticism of our manuscript. The personnel at FCRDC are thanked for their assistance. The research of R. N. in Israel has been supported in part by grant number 95-00208 from BSF, Israel, by a grant from the Israel Science Foundation administered by the Israel Academy of Sciences, by the Magnet grant, by the Ministry of Science grant, and by the Tel Aviv University Basic Research and Adams Brain Center grants. This project has been funded in whole or in part with Federal funds from the National Cancer Institute, National Institutes of Health, under contract number NO1-CO-56000. The content of this publication does not necessarily reflect the view or policies of the Department of Health and Human Services, nor does mention of trade names,

commercial products, or organization imply endorsement by the US Government.

References

Baldwin, R. L. & Rose, G. D. (1999). Is protein folding hierarchic? II. Folding intermediates and transition states. *Trends Biochem. Sci.* **24**, 77-84.

Barlow, D. J. & Thornton, J. M. (1983). Ion-pairs in proteins. *J. Mol. Biol.* **168**, 867-885.

Barril, X., Aleman, C., Orozco, M. & Luque, F. J. (1998). Salt bridge interactions: stability of ionic and neutral complexes in the gas phase, in solution and in proteins. *Proteins: Struct. Funct. Genet.* **32**, 67-79.

Bernstein, F., Koetzle, T., Williams, G., Meyer, E. J., Brice, M., Rodgers, J., Kennard, O., Shimanuchi, T. & Tasumi, M. (1977). The Protein Data Bank: a computer based archival file for macromolecular structures. *J. Mol. Biol.* **112**, 535-542.

Dao-pin, S., Anderson, D. E., Baase, W. A., Dahlquist, F. W. & Matthews, B. W. (1991). Structural and thermodynamic consequences of burying a charged residue within the hydrophobic core of T4 lysozyme. *Biochemistry,* **30**, 11521-11529.

deBakker, P. I. W., Hunenberger, P. H. & McCammon, J. A. (1999). Molecular dynamics simulations of the hyperthermophilic protein Sac7d from *Sulfolobus acidocaldarius*: contribution of salt bridges to thermostability. *J. Mol. Biol.* **285**, 1811-1830.

Elcock, A. H. (1998). The stability of salt bridges at high temperatures: implications for hyperthermophilic proteins. *J. Mol. Biol.* **284**, 489-502.

Fersht, A. R. (1972). Conformational equilibria in α- and δ- chymotrypsin. The energetics and importance of the salt bridge. *J. Mol. Biol.* **64**, 497-509.

Gilson, M. K. & Honig, B. H. (1987). Calculation of electrostatic potential in an enzyme active site. *Nature,* **330**, 84-86.

Gilson, M. K. & Honig, B. H. (1988). Calculation of the total electrostatic energy of a macromolecular system: solvation energies, binding energies, and conformational analysis. *Proteins: Struct. Funct. Genet.* **4**, 7-18.

Gilson, M. K., Rashin, A., Fine, R. & Honig, B. (1985). On the calculation of electrostatic interactions in proteins. *J. Mol. Biol.* **183**, 503-516.

Gilson, M. K., Sharp, K. A. & Honig, B. H. (1988). Calculating the electrostatic potential of molecules in solution: method and error assessment. *J. Comp. Chem.* **9**, 327-335.

Hendsch, Z. S. & Tidor, B. (1994). Do salt bridges stabilize proteins? A continuum electrostatic analysis. *Protein Sci.* **3**, 211-226.

Hendsch, Z. S., Sindelar, C. V. & Tidor, B. (1998). Parameter dependence in continuum electrostatic calculations: a study using protein salt bridges. *J. Phys. Chem. ser. B,* **102**, 4404-4410.

Honig, B. H. & Hubell, W. L. (1984). Stability of ''salt bridges'' in membrane proteins. *Proc. Natl Acad. Sci. USA,* **81**, 5412-5416.

Honig, B. & Nicholls, A. (1995). Classical electrostatics in biology and chemistry. *Science,* **268**, 1144-1149.

Honig, B., Sharp, K. & Yang, A. (1993). Macroscopic models of aqueous solutions: biological and chemical applications. *J. Phys. Chem.* **97**, 1101-1109.

Horovitz, A. & Fersht, A. R. (1992). Co-operative interactions during protein folding. *J. Mol. Biol.* **224**, 733-740.

Kawamura, S., Tanaka, I. & Kimura, M. (1997). Contribution of a salt bridge to the thermostability of DNA binding protein HU from *Bacillus stearothermophilus* determined by site directed mutagenesis. *J. Biochem.* **121**, 448-455.

Klapper, I., Hagstrom, R., Fine, R., Sharp, K. & Honig, B. (1986). Focusing of electric fields in the active site of Cu-Zn superoxide dismutase: effects of ionic strength and amino acid modification. *Proteins: Struct. Funct. Genet.* **1**, 47-59.

Kumar, S. & Bansal, M. (1998). Dissecting α-helices: position specific analysis of α-helices in globular proteins. *Proteins: Struct. Funct. Genet.* **31**, 460-476.

Kumar, S., Tsai, C. J., Ma, B. & Nussinov, R. (1999). Contribution of salt bridges toward protein thermostability. *J. Biomol. Struct. Dynam.* In the press.

Lee, B. K. & Richards, F. M. (1971). The interpretation of protein structures. Estimation of static accessibility. *J. Mol. Biol.* **55**, 379-400.

Lounnas, V. & Wade, R. C. (1997). Exceptionally stable salt bridges in cytochrome P450cam have functional roles. *Biochemistry,* **36**, 5402-5417.

Marqusee, S. & Sauer, R. T. (1994). Contribution of a hydrogen bond/salt bridge network to the stability of secondary and tertiary structures in lambda repressor. *Protein Sci.* **3**, 2217-2225.

Musafia, B., Buchner, V. & Arad, D. (1995). Complex salt bridges in proteins: statistical analysis of structure and function. *J. Mol. Biol.* **254**, 761-770.

Perutz, M. F. (1970). Stereochemistry of cooperative effects in haemoglobin. *Nature,* **228**, 726-739.

Pervushin, K., Billeter, M., Siegal, G. & Wuthrich, K. (1996). Structural role of a buried salt bridge in the 434 repressor DNA-binding domain. *J. Mol. Biol.* **264**, 1002-1012.

Radzicka, A. & Wolfenden, R. (1988). Comparing the polarities of the amino acids: side-chain distribution coefficients between the vapor phase, cylclohexane, 1-octanol and neutral aqueous solution. *Biochemistry,* **27**, 1664-1670.

Serrano, L., Horovitz, A., Avron, B., Bycroft, M. & Fersht, A. R. (1990). Estimating the contribution of engineered surface electrostatic interactions to protein stability by using double mutant cycles. *Biochemistry,* **29**, 9343-9352.

Sharp, K. A. & Honig, B. (1990). Electrostatic interactions in macromolecules: theory and applications. *Annu. Rev. Biophys. Biophys. Chem.* **19**, 301-332.

Singh, U. C. (1988). Probing the salt bridge in the dihydrofolate reductase-methotrexate complex by using the coordinate-coupled free energy perturbation method. *Proc. Natl Acad. Sci. USA,* **85**, 4280-4284.

Sitkoff, D., Sharp, K. A. & Honig, B. (1994). Accurate calculation of hydration free energies using macroscopic solvent models. *J. Phys. Chem.* **98**, 1978-1988.

Sun, D. P., Sauer, U., Nicholson, H. & Matthews, B. W. (1991). Contributions of engineered surface salt bridges to the stability of T4 lysozyme determined by directed mutagenesis. *Biochemistry,* **30**, 7142-7153.

Spek, E. J., Bui, A. H., Lu, M. & Kallenbach, N. R. (1998). Surface salt bridges stabilize the GCN4 leucine zipper. *Protein Sci.* **11**, 2431-2437.

Tsai, C. J. & Nussinov, R. (1997). Hydrophobic folding units derived from dissimilar monomer structures and their interactions. *Protein Sci.* **6**, 24-42.

Tsai, C. J., Lin, S. L., Wolfson, H. & Nussinov, R. (1996). A dataset of protein-protein interfaces generated

with a sequence order independent comparison technique. *J. Mol. Biol.* **260**, 604-620.
Tsai, C. J., Lin, S. L., Wolfson, H. J. & Nussinov, R. (1997). Studies of protein-protein interfaces: a statistical analysis of the hydrophobic effect. *Protein Sci.* **6**, 53-64.
Tsai, C. J., Kumar, S., Ma, B. & Nussinov, R. (1999). Folding funnels, binding funnels and protein function. *Protein Sci.* **8**, 1179-1188.
Waldburger, C. D., Schildbach, J. F. & Sauer, R. T. (1995). Are buried salt bridges important for protein stability and conformational specificity? *Nature Struct. Biol.* **2**, 122-128.
Waldburger, C. D., Jonsson, T. & Sauer, R. T. (1996). Barriers to protein folding: formation of buried polar interactions is a slow step in acquisition of structure. *Biochemistry,* **93**, 2629-2634.
Xiao, L. & Honig, B. (1999). Electrostatic contributions to the stability of hyperthermophilic proteins. *J. Mol. Biol.* **289**, 1435-1444.
Xu, D., Tsai, C. J. & Nussinov, R. (1997a). Hydrogen bonds and salt bridges across protein-protein interfaces. *Protein Eng.* **10**, 999-1012.
Xu, D., Lin, S. L. & Nussinov, R. (1997b). Protein binding versus protein folding: the role of hydrophilic bridges in protein associations. *J. Mol. Biol.* **265**, 68-84.
Yip, K. S. P., Britton, K. L., Stillman, T. J., Lebbink, J., De Vos, W. M., Robb, F. T., Vetriani, C., Maeder, D. & Rice, D. W. (1998). Insights into the molecular basis of thermal stability from the analysis of ion pair networks in the glutamate dehydrogenase family. *Eur. J. Biochem.* **255**, 336-346.

Edited by J. M. Thornton

(Received 8 June 1999; received in revised form 20 September 1999; accepted 20 September 1999)

http://www.academicpress.com/jmb

Supplementary material comprising one Table is available from JMB Online.